Supporting Information

Magnesium Stabilized Multifunctional DNA Nanoparticles for Tumor-Targeted and pH-Responsive Drug Delivery

*Haoran Zhao[a], Xuexia Yuan[a], Jiantao Yu[a], Yishun Huang[a], Chen Shao[a], Fan Xiao[a], Li Lin[a], Yan Li[b] and Leilei Tian[a]**

[a] Department of Materials Science and Engineering, Southern University of Science and Technology, 1088 Xueyuan Blvd., Nanshan District, Shenzhen, Guangdong 518055, P. R. China.

[b] Department of Biology, Southern University of Science and Technology, 1088 Xueyuan Blvd., Nanshan District, Shenzhen, Guangdong 518055, P. R. China.

* Email: tianll@sustc.edu.cn.

Table S1. DNA Sequences used in this work.

H1	5′-CGC CCC TAA CCC TAA CCC TAA CCC TGC G
H2	5′-CGC CGC CCC TAA CCC TAA CCC TAA CCC TGC GGC G
H3	5′-CGC AGC CCC TAA CCC TAA CCC TAA CCC TGC TGC G
H4	5′-AAC GCG CCC TAA CCC TAA CCC TAA CCC TCG CGT T
H5	5′- GA TCG TAT CCC TAA CCC TAA CCC TAA CCC ATA CGA TC
H6	5′- GA TCG TAT TCG CCC TAA CCC TAA CCC TAA CCC CGA ATA CGA TC
H7	5′- GA TCG TAT TCG TAT TCG CCC TAA CCC TAA CCC TAA CCC CGA ATA CGA ATA CGA TC
T1 (Sgc8)	5′-CG GCG GCG CAG CAG TTA GAT TTT TGA TCG TAT GGG TTA GGG TTA GGG TTA GGG ATA CGA TCT TTT TCT AAC CGT ACA GTA TTT TCC
T2 (nonsgc8)	5′-CG GGC TTA CTT ACT TAC ACT TTT TGA TCG TAT GGG TTA GGG TTA GGG TTA GGG ATA CGA TCT TTT CAC AGG CTT CAG GGC TTA CAC
U1	5′-GGA AAA TAC TGT ACG GTT AGA AAA AGA TCG TAT CCC TAA CCC TAA CCC TAA CCC ATA CGA TCA AAA ATC TAA CTG CTG CGC CGC CG

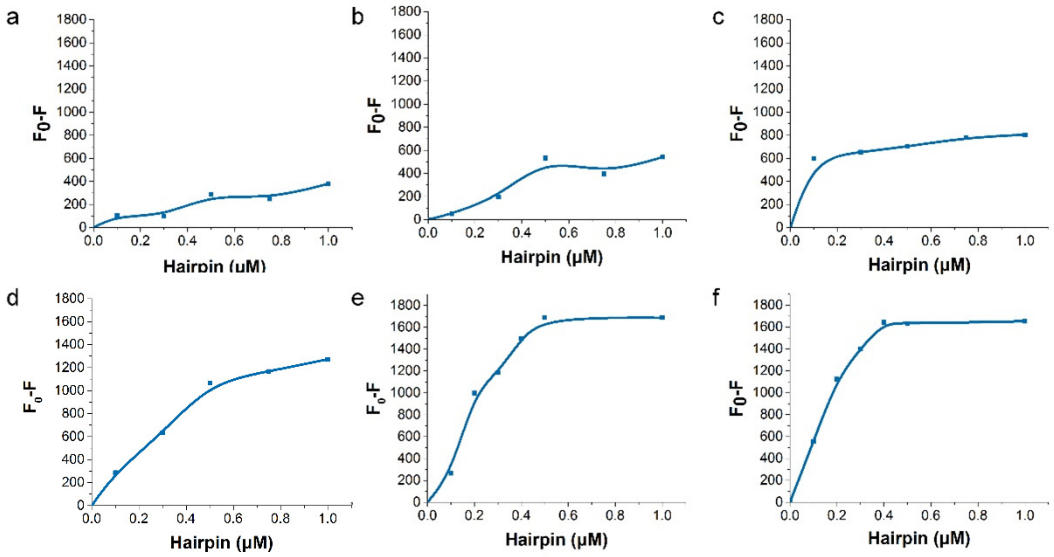

Figure S1. Dox loading capability of H1 (a); H2 (b); H3 (c); H4 (d); H6 (e); H7 (f). In this experiment, different amounts of DNA hairpin were titrated to a solution of 2 μM Dox in 1×PBS buffer (pH 7.4), and the resultant fluorescence intensities were recorded.

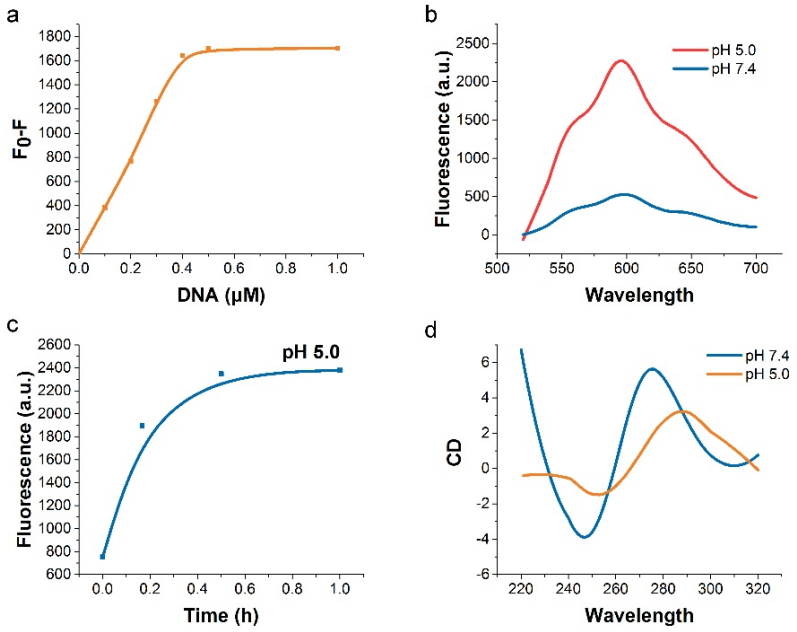

Figure S2. Dox loading and release properties of H5. (a) Dox loading capability in presence of 2 μM Dox; (b) the fluorescence spectra of Dox (2 μM), when Dox was fully loaded in H5 at pH 7.4 (the blue line) and at pH 5.0 (the red line), respectively. (c) The Dox release from H5 when pH was switched to 5.0. (d) CD spectra of H5 at different pH values.

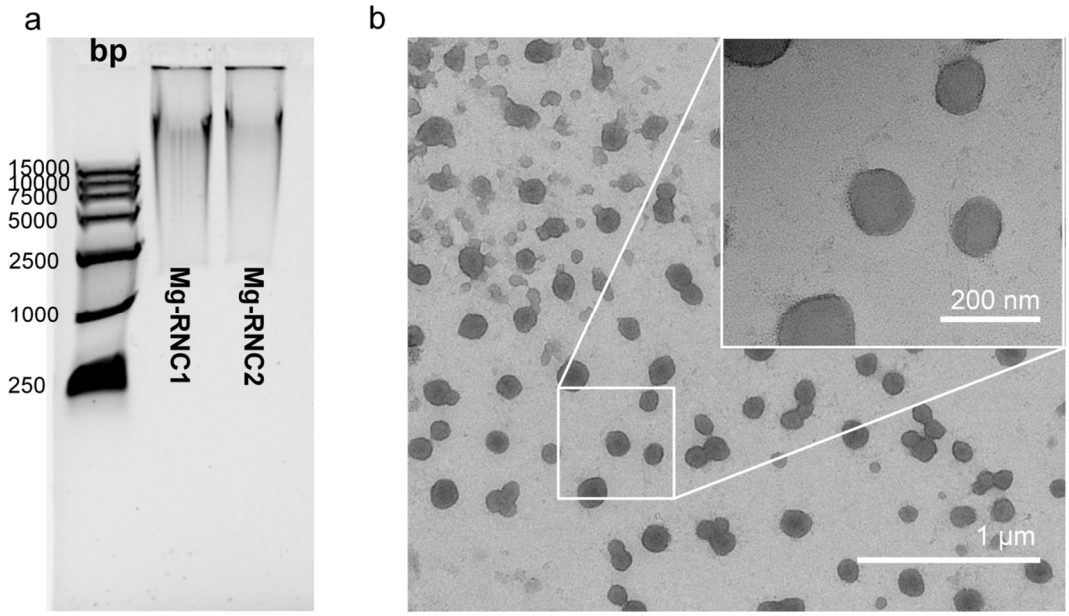

Figure S3. (a) Agarose gel electrop.horesis analysis for RCA1 and RCA2, which were amplified from T1 and T2, respectively; (b) TEM image of Mg-RNC2.

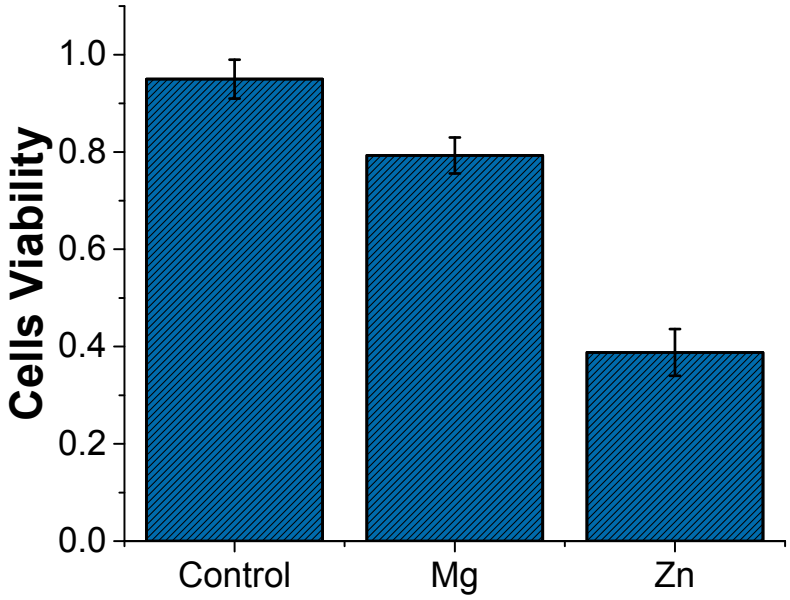

Figure S4. Cytotoxicity of Mg^{2+} and Zn^{2+}(38 μM) that co-cultured with CEM for 24 h.

Table S2. Laser light scattering (LLS) data of U1 condensed by Mg^{2+}

	Rh(nm)	Rg(nm)	Rg/Rh	Structure
Mg/P=200	147.6	219.2	1.4851	Gaussian coil, monodisperse

Table S3. Zeta potential of RCA products in presence of different amounts of Mg^{2+}.

Mg/P	Zeta potential (mV)
0:1	-37.145
100:1	-8.63
200:1	-5.51
400:1	2.66

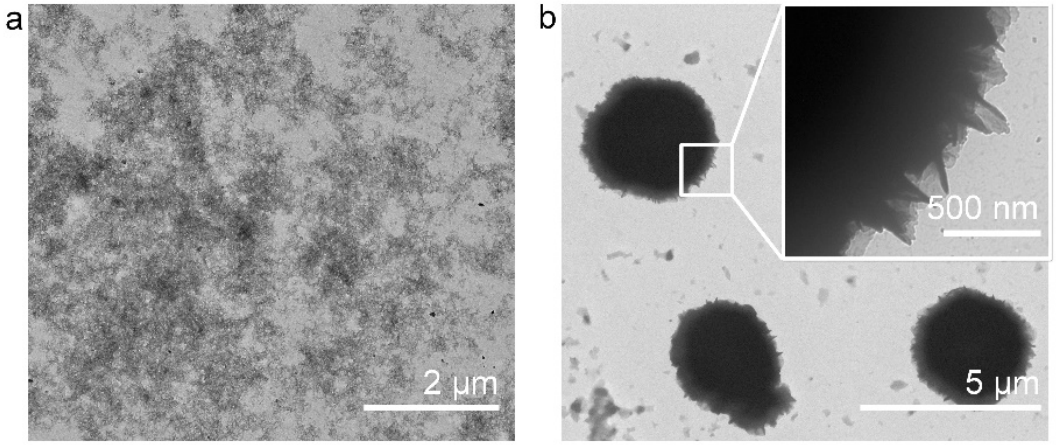

Figure S5. TEM images of (a) the purified RCA products (long ssDNA) and (b) *in situ* formed MgPPi-RNC.

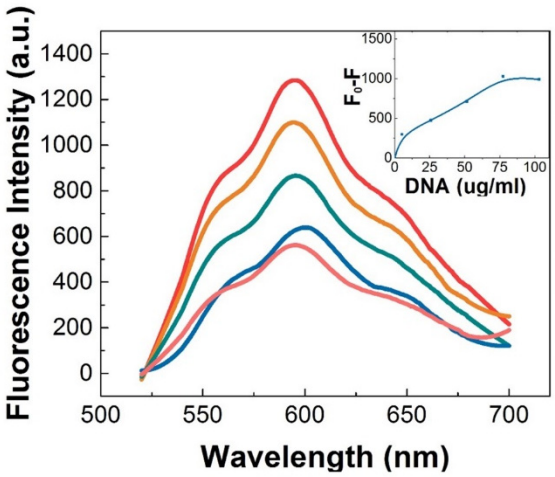

Figure S6. The fluorescence of Dox (2 μM) mixed with different concentrations of MgPPi-RNC (whose concentration is determined by the incorporated DNAs); the insert gives the relationship between fluorescence changes and DNA concentrations.

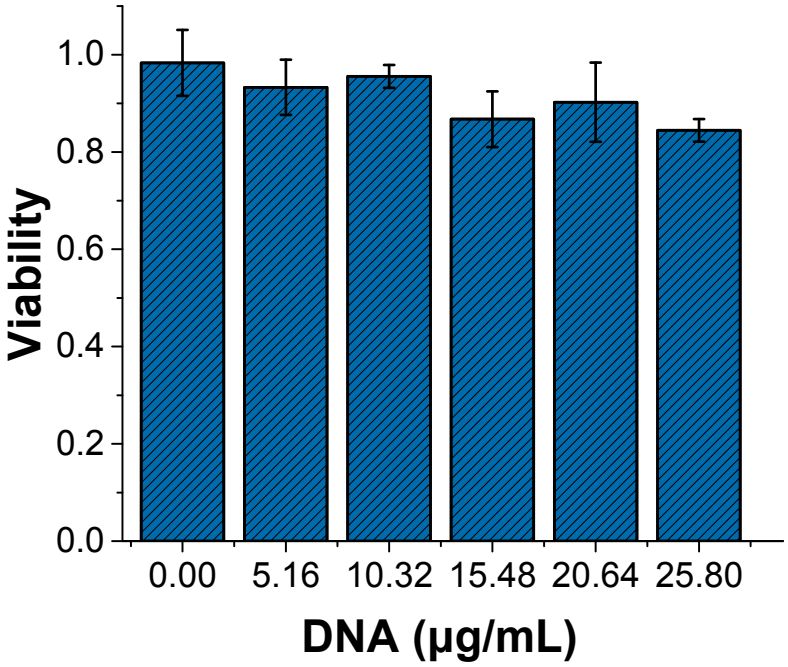

Figure S7. Cytotoxicity of Mg-RNC1 for CEM cells**.**

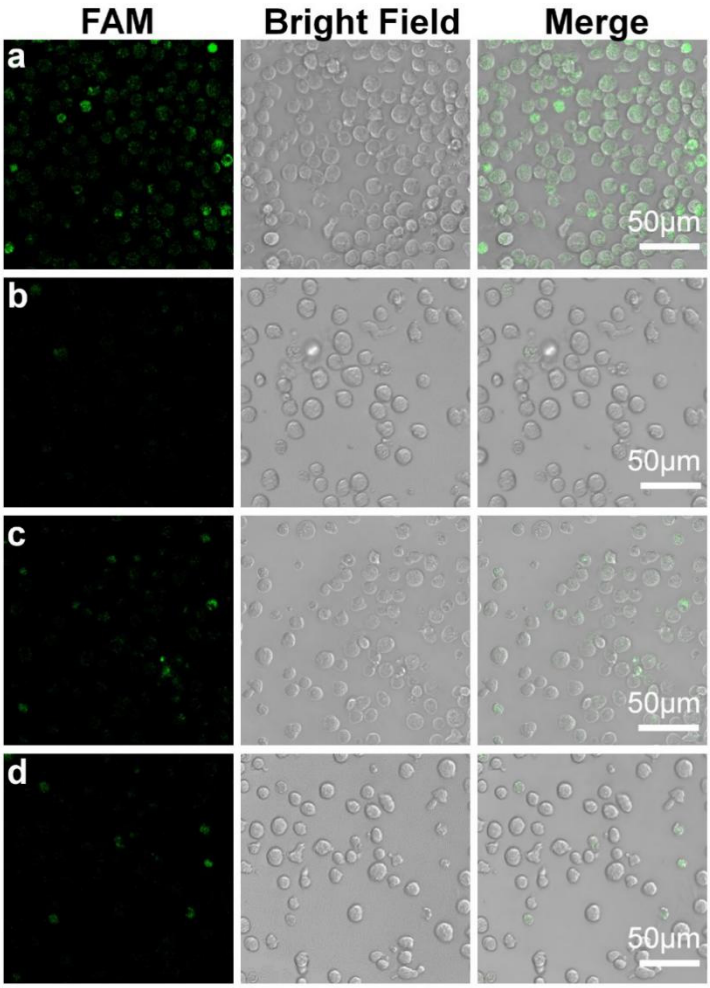

Figure S8. LSCM images of (a) CEM cells co-cultured with Mg-RNC1; (b): Ramos cells co-cultured with Mg-RNC1; (c) CEM cells co-cultured with Mg-RNC2; (d) Ramos cells co-cultured with Mg-RNC2.

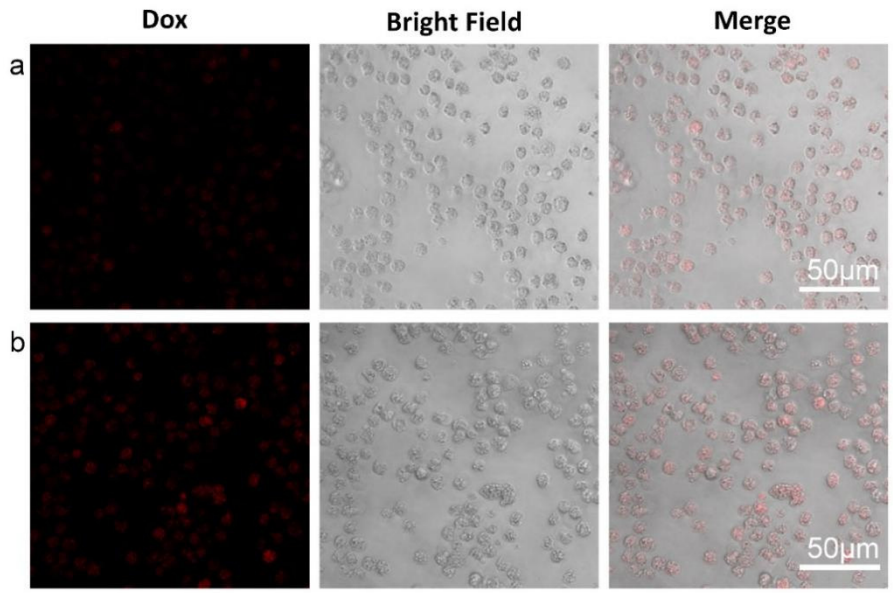

Figure S9. LSCM images of Ramos cells incubated with (a) Mg-RNC2@Dox and (b) free Dox.

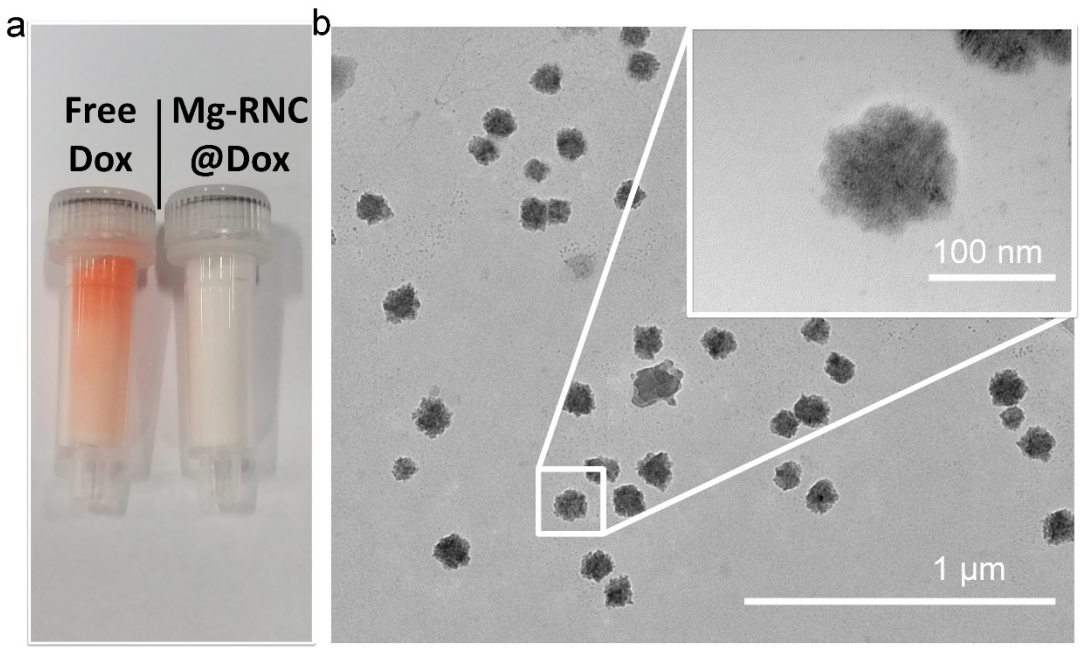

Figure S10. (a) A photo of two salt-removal columns after the treatment with free Dox and Mg-RNC@Dox, respectively. (b) TEM images of Mg-RNC1@Dox after the salt removal treatment.

Mg^{2+} content in the nanoparticle and the dynamic release of Mg^{2+} during incubation

Table S4. Mg^{2+} content in Mg-RNCs and MgPPi-RNCs.

Samples	MgPPi-RNCs	Mg-RNCs (raw)	Mg-RNCs (desalted)
Mg^{2+} content (mol Mg^{2+}/0.1 g DNA)	0.005115	0.056859	0.001346

Mg-RNC nanoparticles were desalted through desalting column prior to *in vivo* applications. As shown in Figure S10, the Mg-RNCs can still keep intact and stable after go through the desalting column. Inductively coupled plasma mass spectrometry (ICP-MS) was utilized here to test the content of Mg^{2+} in MgPPi-RNCs, raw Mg-RNCs, and desalted Mg-RNCs. As shown in Table S4, for every 0.1 g DNA in the nanoparticles, MgPPi-RNCs contains ~5.1 mmol Mg^{2+} and desalted Mg-RNCs contains ~1.3 mmol Mg^{2+}; and before salt removal treatment, raw Mg-RNCs contains 56.9 mmol Mg^{2+}, indicating a majority part of Mg^{2+} has been removed after the desalting treatment. These results demonstrated that although an excessive amount of Mg^{2+} was required to drive DNA condensation; once the condensation formed, Mg-RNCs would be stabilized by the interior Mg^{2+}, whose structure would not be affected by the removal of exterior ions.

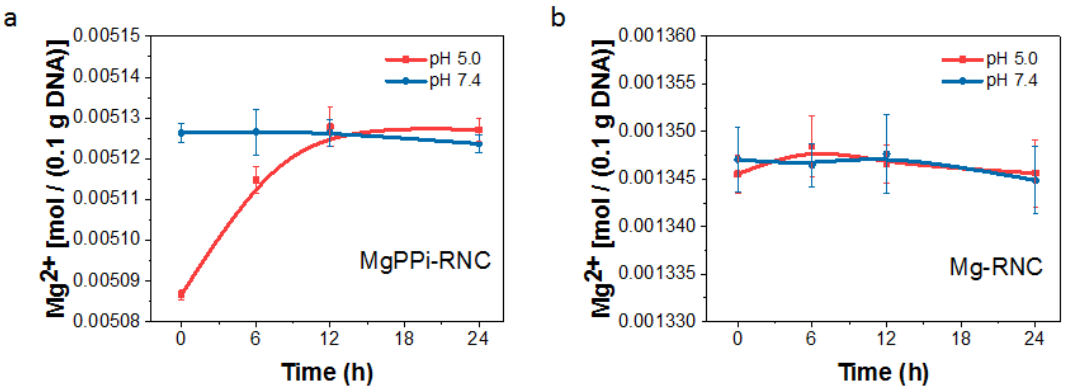

Figure S11. Dynamic changes of Mg^{2+} content in MgPPi-RNCs (a) and desalted Mg-RNCs (b) during a 24-h incubation at pH 7.4 and pH 5.0, respectively.

Mg-RNCs and MgPPi-RNCs were incubated in PBS buffers of pH 7.4 and pH 5.0

for different periods of time, and the samples were characterized by ICP-MS to analyze the dynamic release of Mg^{2+} from the two kinds of nanoparticles. As shown in Figure C6a, for MgPPi-RNCs, there was very few Mg^{2+} was released from the nanoparticles after 24 h incubation in buffer of pH 7.4; on the other side, in buffer of pH 5.0, a small amount (< 1%) was released from MgPPi-RNCs at the very beginning, which was gradually re-absorbed into the nanoparticles during the 24 h incubation process. The release at the beginning of the incubation at pH 5.0 is probably because of the dissolution of MgPPi on the surface of MgPPi-RNCs at the acidic condition. As shown in Figure C6b, no matter incubated at pH 7.4 or pH 5.0, both situations exhibited negligible Mg^{2+} releases from Mg-RNCs during the 24 h process. Therefore, we can conclude that the electrostatic interaction between DNAs and Mg^{2+} is very strong, which, on one side, stabilizes the condensation structures of DNA nanoparticles, and moreover, avoids Mg^{2+} release from the nanoparticles, ensuring good biocompatibility and lower toxicity of this kind of DNA nanoparticles.

Sample preparation and ICP-MS analysis: MgPPi-RNCs and Mg-RNCs were fabricated under the same concentration of DNA (0.1 mg/mL). The dispersed solutions of MgPPi-RNC and Mg-RNC were adjusted to pH 7.4 or pH 5.0, which were processed to different incubation time. (1) Total content of Mg^{2+}: Nitric acid (5%, ~1.1 M) was added to the samples and heated the samples to 95 °C for 10 min to denature DNA and acquire pure Mg^{2+}; (2) Content of free Mg^{2+}: Thereafter, the samples were filtered by ultrafiltration tubes to retain DNA nanoparticles, and flow-through parts containing free Mg^{2+} were collected. Nitric acid (5%, ~1.1 M) was added to the collected samples prior to ICP-MS analysis.

ICP-MS analysis: Samples were diluted sufficiently and detected *via* ICP-MS (Agilent 7700X) and calculated by standard curve of Mg^{2+}. The Mg^{2+} content in nanoparticles ($C_{nanoparticle}$) were calculated by the following formula according to the total content (C_{total}) and the content of free Mg^{2+} (C_{free}):

$$C_{nanoparticle} = C_{total} - C_{free}$$